Bioactive Materials 6 (2021) 4321–4332

Contents lists available at ScienceDirect

Bioactive Materials

journal homepage: www.sciencedirect.com/journal/bioactive-materials

Isolation of cabbage exosome-like nanovesicles and investigation of their biological activities in human cells

Jae Young You [a,1], Su Jin Kang [a,1], Won Jong Rhee [a,b,*]

[a] Department of Bioengineering and Nano-Bioengineering, Incheon National University Incheon, 22012, Republic of Korea
[b] Division of Bioengineering, Incheon National University Incheon 22012, Republic of Korea

ARTICLE INFO

Keywords:
Exosome-like nanovesicles
Cabbage
Inflammation
Apoptosis
Drug delivery

ABSTRACT

There are extensive studies on the applications of extracellular vesicles (EVs) produced in cell culture for therapeutic drug development. However, large quantities of EVs are needed for *in vivo* applications, which requires high production costs and time. Thus, the development of new EV sources is essential to facilitate their use. Accordingly, plant-derived exosome-like nanovesicles are an emerging alternative for culture-derived EVs. Until now, however, few studies have explored their biological functions and uses. Therefore, it is necessary to elucidate biological activities of plant-derived exosome-like nanovesicles and harness vesicles for biomedical applications. Herein, cabbage and red cabbage were used as nanovesicle sources owing to their easy cultivation. First, an efficient method for nanovesicle isolation from cabbage (Cabex) and red cabbage (Rabex) was developed. Furthermore, isolated nanovesicles were characterized, and their biological functions were assessed. Both Cabex and Rabex promoted mammalian cell proliferation and, interestingly, suppressed inflammation in immune cells and apoptosis in human keratinocytes and fibroblasts. Finally, therapeutic drugs were encapsulated in Cabex or Rabex and successfully delivered to human cells, demonstrating the potential of these vesicles as alternative drug delivery vehicles. Overall, the current results provide strong evidence for the wide application of Cabex and Rabex as novel therapeutic biomaterials.

1. Introduction

Extracellular vesicles (EVs) are particles produced by various cells, ranging from microbial and plant to human cells [1]. They facilitate cell-to-cell communication through the transfer of encapsulated bioactive molecules, including DNA, RNA, proteins, and lipids [2,3]. Exosomes are the smallest particles among EVs with sizes ranging from 50 to 150 nm and are enriched in the body fluids, including blood, saliva, urine, and breast milk [4–6]. As central mediators of intercellular communication, EVs, including exosomes, play important roles in the pathogenesis of various diseases, including cancer progression and metastasis [7,8]. Recent studies have demonstrated the therapeutic potential of EVs produced by human cells [9–11]. For instance, mesenchymal stem cell-derived EVs have been shown to modulate cell proliferation and regeneration of damaged tissue [12]. In addition, owing to their small size, EVs produced from cell cultures can successfully deliver therapeutic agents, such as proteins, peptides, small molecules, and nucleic acids, to cells [13,14]. However, a crucial disadvantage of using cell culture derived EVs is that clinical applications of EVs in humans require a huge number of EVs. To provide such numbers, large-scale cell culture derived EV production is necessary, which requires high production costs and time. Further, mammalian cell cultures require the use of animal-derived components, such as fetal bovine serum (FBS), which is generally prohibited for drug approval due to safety concerns. Conclusively, alternative EV sources are required to overcome these issues.

Recently, plant-derived exosome-like nanovesicles have gained huge attention as potential therapeutic effects such as anti-cancer, anti-melanogenic, and anti-inflammatory activities that can help maintain the homeostasis. There have been several interesting reports on plant-derived exosome-like nanovesicle development for the treatment of disease, especially in the human colon [15,16]. Grape exosome-like nanoparticles successfully targeted intestinal stem cells after oral uptake and protected mice from colitis [17]. Nanovesicles derived from

Peer review under responsibility of KeAi Communications Co., Ltd.
* Corresponding author. Division of Bioengineering, Incheon National University Incheon 22012, Republic of Korea.
E-mail address: wjrhee@inu.ac.kr (W.J. Rhee).
[1] These authors contributed equally to this work.

https://doi.org/10.1016/j.bioactmat.2021.04.023
Received 29 December 2020; Received in revised form 18 March 2021; Accepted 10 April 2021

edible ginger were successfully taken up by intestinal epithelial cells and macrophages following oral administration, drastically alleviating acute colitis and preventing chronic colitis as well as colitis-associated cancer [18]. Blueberry-derived nanoparticles were able to modulate the expression of genes involved in inflammatory response, cytokine release, and oxidative stress [19]. Recently, exosome-like particles from strawberry were shown to prevent oxidative stress in human cells by delivering intrinsic vitamin C [20]. Lemon-derived nanoparticles have *in vitro* anti-neoplastic activity on a panel of different solid and hematological cancers cell lines [21]. Thus, plant exosome-like nanovesicles have potential as therapeutic drugs and drug delivery vehicles for the treatment of disease [22–24]. However, nanovesicles derived from plants have not been extensively studied despite their potential, even though EVs produced from plant cells were discovered earlier than mammalian cell-derived EVs [25]. There are a limited number of studies investigating the physiological effects of these plant nanovesicles in humans. In addition, there is no standard method for exosome-like nanovesicle isolation from plants, ensuring high yield and purity.

Herein, cabbage and red cabbage were introduced as new sources of plant exosome-like nanovesicles that are easily and widely cultivated, allowing for lower nanovesicle production costs and shorter production times (Fig. 1). First, nanovesicle isolation processes were developed to yield a high amount of exosome-like nanovesicles with high purity. We used size-exclusion chromatography combined with ultrafiltration for exosome-like nanovesicles isolation from cabbage and red cabbage, and nanovesicle yield and purity were compared to those of other isolation methods. The physiological effects of exosome-like nanovesicles isolated from cabbage (Cabex) and red cabbage (Rabex) in mammalian cells were then investigated, especially with regard to proliferation, regulation of inflammation, and inhibition of apoptosis. Finally, to overcome challenges associated with cell culture-derived EVs, the drug delivery capacities of Cabex and Rabex were explored in order to demonstrate their potential as drug delivery vehicles and determine whether they can be an alternative to cell culture-derived EVs. The results of the current study provide strong evidence that plant-derived exosome-like nanovesicles are novel therapeutic biomaterials with potential for wide biomedical application.

2. Results and discussion

2.1. Isolation of exosome-like nanovesicles from cabbage using ultrafiltration and size-exclusion chromatography

To investigate the biological and pharmacological activities of Cabex and Rabex, it is necessary to isolate plant-derived nanovesicles from cabbage with high yield and purity. PEG-based precipitation and ultracentrifugation, both of which are widely available, have been recently applied as tools for nanovesicle isolation from plants [26]. Precipitation methods have been criticized as their yields are accompanied by high levels of protein impurities [27]. Ultracentrifugation provides low EV yields because a large number of nanovesicles are lost during centrifugation. Moreover, it is possible that protein aggregates are retained, and nanovesicles are disrupted due to high centrifugal forces, which may complicate the application of isolated nanovesicles [28,29]. In this context, size-exclusion chromatography combined with ultrafiltration was introduced to isolate nanovesicles from cabbage. The same amount of cabbage was also used for nanovesicle isolation using ultracentrifugation and PEG-based precipitation methods for comparison. Cabbage or red cabbage juices containing nanovesicles were concentrated using ultrafiltration to reduce the volume before injection into the size-exclusion chromatography column for isolation. The nanovesicle concentrations and size distributions were analyzed using NTA, and protein (impurity) concentrations in each size-exclusion chromatography fraction were measured [30]. As shown in Fig. 2A, a high concentration of nanovesicles was collected in fractions 7 to 10, while most protein impurities were separated and collected in fractions 13 to 30, indicating that Cabex was successfully separated from the majority of protein contaminants. Thus, fractions 7 to 10 were collected as Cabex because they contained high nanovesicle amounts with minimal protein contamination. A similar nanovesicle isolation pattern was observed for red cabbage (Fig. 2B). Fractions 6 to 9 were collected as Rabex and further used for characterization.

The size distributions of Cabex and Rabex isolated using 3 different methods were analyzed by NTA (Fig. 2C–H). Interestingly, nanovesicles isolated by ultracentrifugation and PEG-based precipitation showed multiple peaks, indicating that there were heterogeneous nanoparticles of various sizes. On the contrary, nanovesicles isolated by size exclusion chromatography showed a relatively homogeneous peak, indicating pure nanovesicles isolated from cabbage and red cabbage (Fig. 2C–H). The average sizes of isolated nanovesicles were 148.2, 134.2, and 98.8 nm for PEG precipitation, ultracentrifugation, and size-exclusion chromatography, respectively (Fig. 2I). Cabex yield and purity were also assessed and compared between isolation methods (Fig. 2J and K). NTA and standard colorimetric protein assay were used to evaluate the purity and yield of Cabex and Rabex. The yield (particles mL^{-1}) was calculated by measuring the vesicle concentrations from the main fractions (Fractions 7 to 10 for Cabex and 6 to 9 for Rabex) in the size exclusion chromatography. The purity (particles μg^{-1} protein) was evaluated by

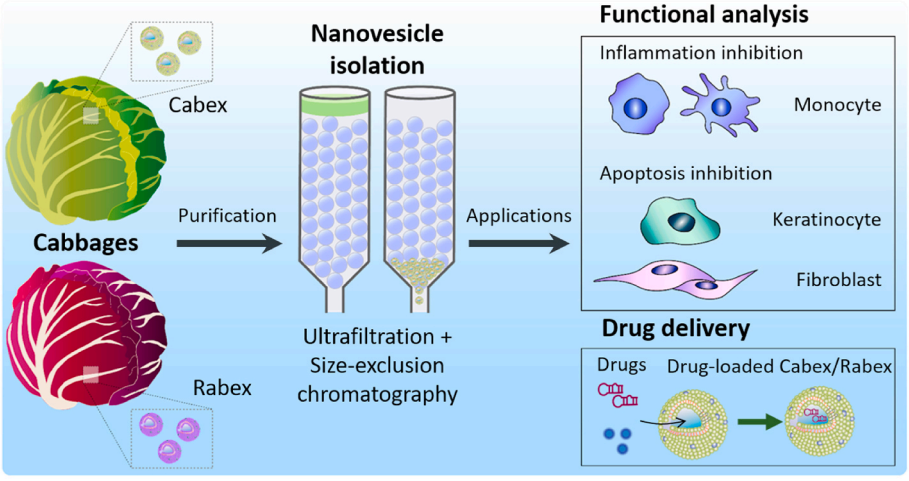

Fig. 1. Schematic illustration of exosome-like nanovesicle isolation from cabbage and the investigation of molecular functions (inflammation and apoptosis inhibition) and applications (drug delivery) of Cabex and Rabex.

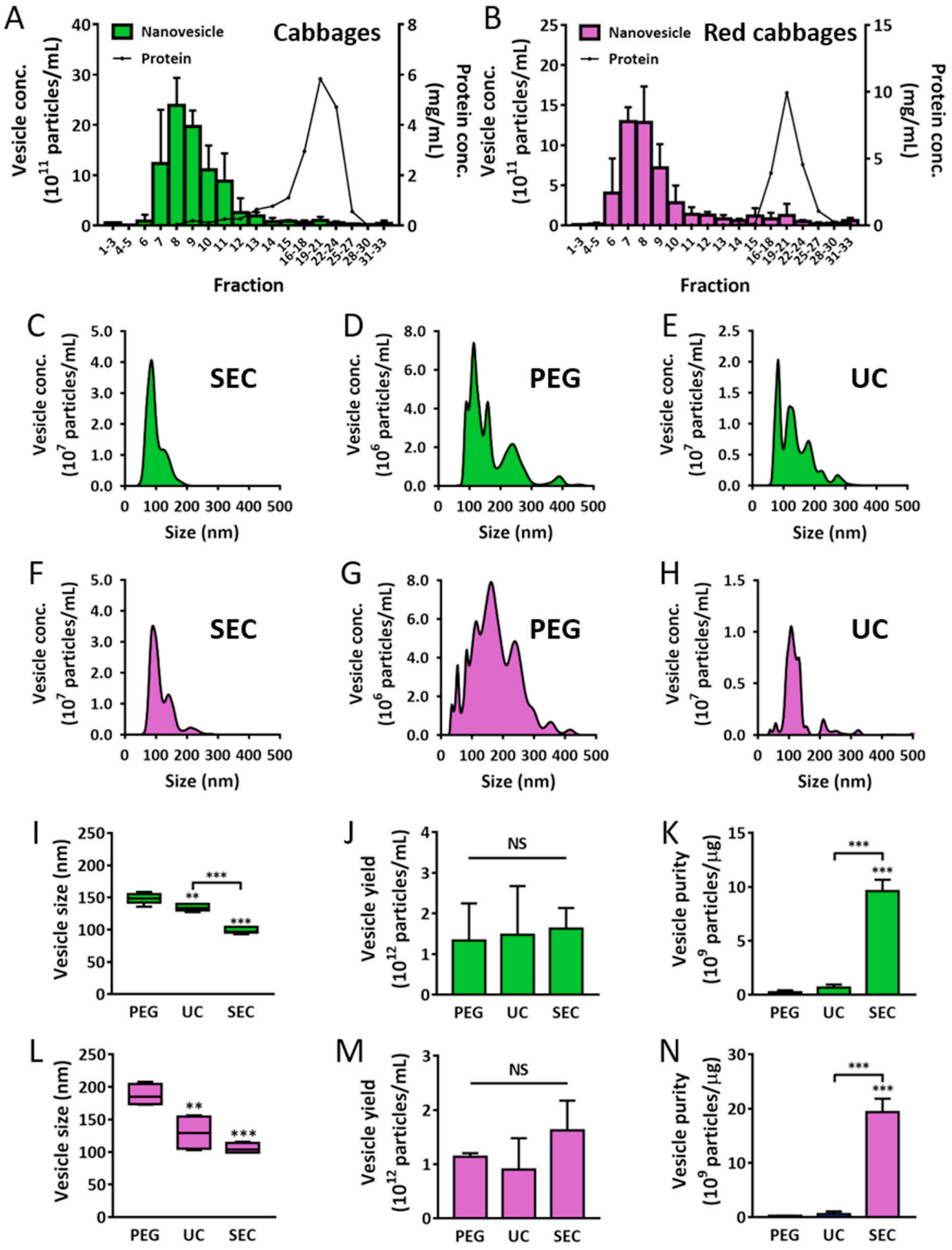

Fig. 2. Isolation of nanovesicles from cabbage and red cabbage. (A) Cabex or (B) Rabex were isolated and purified from cabbage or red cabbage, respectively, using size-exclusion chromatography combined with ultrafiltration. Nanovesicle and protein concentrations in all size-exclusion chromatography fractions were measured. Nanovesicle-containing fractions were used for further characterization. (C–E) Representative size distribution profiles of Cabex isolated by (C) size-exclusion chromatography (SEC), (D) PEG-based precipitation (PEG), and (E) ultracentrifugation (UC) analyzed by NTA. (F–H) Representative size distribution profiles of Rabex isolated by (F) SEC, (G) PEG, and (H) UC analyzed by NTA. (I–K) Comparison of (I) average size, (J) EV yield, and (K) nanovesicle purity of Cabex between isolation methods. (L–N) Comparison of (L) average size, (M) nanovesicle yield, and (N) nanovesicle purity of Rabex between isolation methods. All values are expressed as mean ± SD (**$p < 0.01$, ***$p < 0.001$, NS: not significant; $n = 3$). (For interpretation of the references to color in this figure legend, the reader is referred to the Web version of this article.)

dividing Cabex or Rabex concentration by the protein concentration in the main fractions. There was no statistically significant difference, meaning that the Cabex yields from the same amount of cabbage were similar between methods. However, in terms of purity, Cabex isolation by size-exclusion chromatography was superior to other methods (Fig. 2K). The Cabex purity value for size exclusion chromatography was 10×10^9 particles μg^{-1} protein, while those for PEG and ultracentrifugation were 0.242×10^9 and 0.432×10^9 particles μg^{-1} protein, respectively. Similar patterns were observed for nanovesicles isolated from red cabbage (Fig. 2L–N). As our combined method provided the highest purity without losing yield, size-exclusion chromatography-based isolation can be chosen as a standard method for plant nanovesicle isolation. The method is not limited to nanovesicle isolation from cabbage, but can also be applied for other types of plants. High nanovesicle yields with fewer impurities can also be isolated from cucumbers, peppers, and tomatoes using size-exclusion chromatography combined with ultrafiltration (Fig. S1). nanovesicle yields were different between plants: 1.119×10^{10} particles were obtained from 1 g of tomatoes, while 1.504×10^{11} particles and 1.098×10^{11} particles were obtained from 1 g of cabbage and red cabbage, respectively. Thus, our method can be widely used as a standard method for nanovesicle isolation from plants.

2.2. Characterization of exosome-like nanovesicles from cabbage using size-exclusion chromatography

The characteristics of plant exosome-like nanovesicles were analyzed after isolation by size-exclusion chromatography. The morphological characteristics of Cabex and Rabex were analyzed by TEM. Both nanovesicles showed spherical shapes with an average size of 100 nm (Fig. 3A and B). The average zeta potentials of Cabex and Rabex were −14.8 mV and −15.2 mV, respectively, meaning they were negatively charged, and there was no significant difference between the nanovesicles (Fig. 3C).

We further tested whether plant-derived nanovesicles can bind and be taken up by human cells. This is important as nanovesicles should interact with and transfer their molecular contents into cells in order to exert biological effects. To confirm the penetration and localization of nanovesicles in cells, isolated EVs were added to the HaCaT cell culture medium. Cells were incubated with culture medium containing 1.0×10^{11} particles mL^{-1} of Cabex or Rabex, respectively, labeled with PKH67 green dye. Confocal analysis revealed that Cabex and Rabex could be observed in the cell cytosol, and it was concluded that both plant nanovesicles can penetrate human cells (Fig. 3D–F). Thus, both Cabex and Rabex transport molecular cargo from plants to human cells to subsequently regulate target cell biological activities.

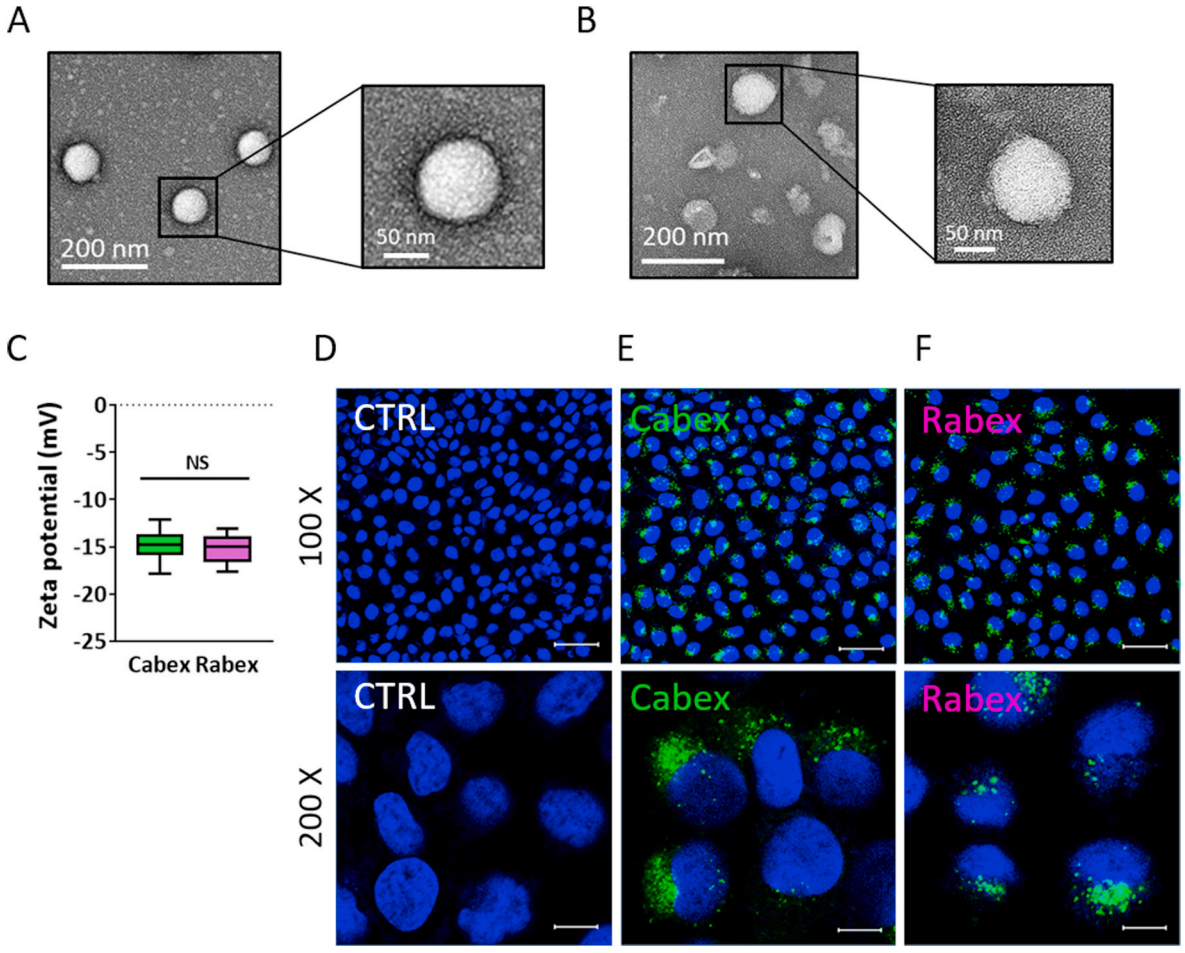

Fig. 3. Characterization of Cabex and Rabex and their intracellular penetration properties. (A, B) Morphology of (A) Cabex and (B) Rabex analyzed by TEM. (C) Zeta potential of Cabex and Rabex. The average zeta potentials of Cabex and Rabex were −14.8 mV and −15.2 mV, respectively. All values are expressed as mean ± SD (NS: not significant; $n = 5$). (D–F) Cabex or Rabex labeled with PKH67 dye were delivered to HaCaT cells. Cells were incubated (D) without EVs (control) and with (E) Cabex or (F) Rabex, and fluorescence images were obtained using a confocal microscope. Green color indicates nanovesicles, and blue color indicates nuclei. The size bars indicate 50 μm (upper panel) and 10 μm (lower panel), respectively. (For interpretation of the references to color in this figure legend, the reader is referred to the Web version of this article.)

2.3. Cytotoxicity and effects of Cabex and Rabex on proliferation in human and mouse cells

Plant-derived exosome-like nanovesicles are natural nanoparticles. In this context, previous studies reported that cytotoxicity of plant-derived exosome-like nanovesicles is low because they originate from cells and are therefore composed of cellular components [16,18,24,31,32]. For instance, grapefruit-derived nanovesicles were successfully uptaken by A549 and CT26 cells without cytotoxicity [33]. Also, no detectable adverse side-effect and cytotoxicity when they were intravenously injected into mice [24]. Oral administration of nanoparticles derived from ginger did not induce the side effects at the local or systemic level in mouse inflammatory bowel disease model [18].

To prove this for Cabex and Rabex, human and mouse cells were used to assess the toxicity. HaCaT and HDF were chosen because they are the representative cells used in many applications, including wound healing [34–38]. RAW264.7 is the most commonly used cell line as *in vitro* model system evaluating the anti-inflammatory activity and safety of natural compound [39–41]. This macrophage generates robust inflammatory responses when challenged by an inflammatory stimulant, including lipopolysaccharide (LPS) [42,43]. To assess the cytotoxicity of Cabex and Rabex, HaCaT, HDF, and RAW264.7 cells were treated with 1×10^{11} and 2×10^{11} particles mL^{-1} of Cabex and Rabex, respectively, and cell viability was measured 72 h after treatment. Although high concentrations of nanovesicles were added to each cell type, there was no significant decrease in cell viability, regardless of cell type and nanovesicle origin (Fig. 4A–C). Thus, the results indicate that Cabex and Rabex are not toxic to human cells.

The effects of plant-derived nanovesicles on cell proliferation were then assessed. Cells were incubated with 0, 1×10^{9}, 1×10^{10}, or 1×10^{11} particles mL^{-1} of Cabex and Rabex, respectively. Cell concentrations were then measured at 0, 24, 48, and 72 h after nanovesicle supplementation. Cabex promoted the proliferation of HaCaT and RAW 264.7 cells 72 h after treatment, but did not affect cell proliferation of HDFs (Fig. 4D–F). Rabex exhibited a stronger effect on cell proliferation, regardless of cell type (Fig. 4G–I). Overall, it was concluded that Cabex and Rabex enhanced cell proliferation without causing cytotoxicity.

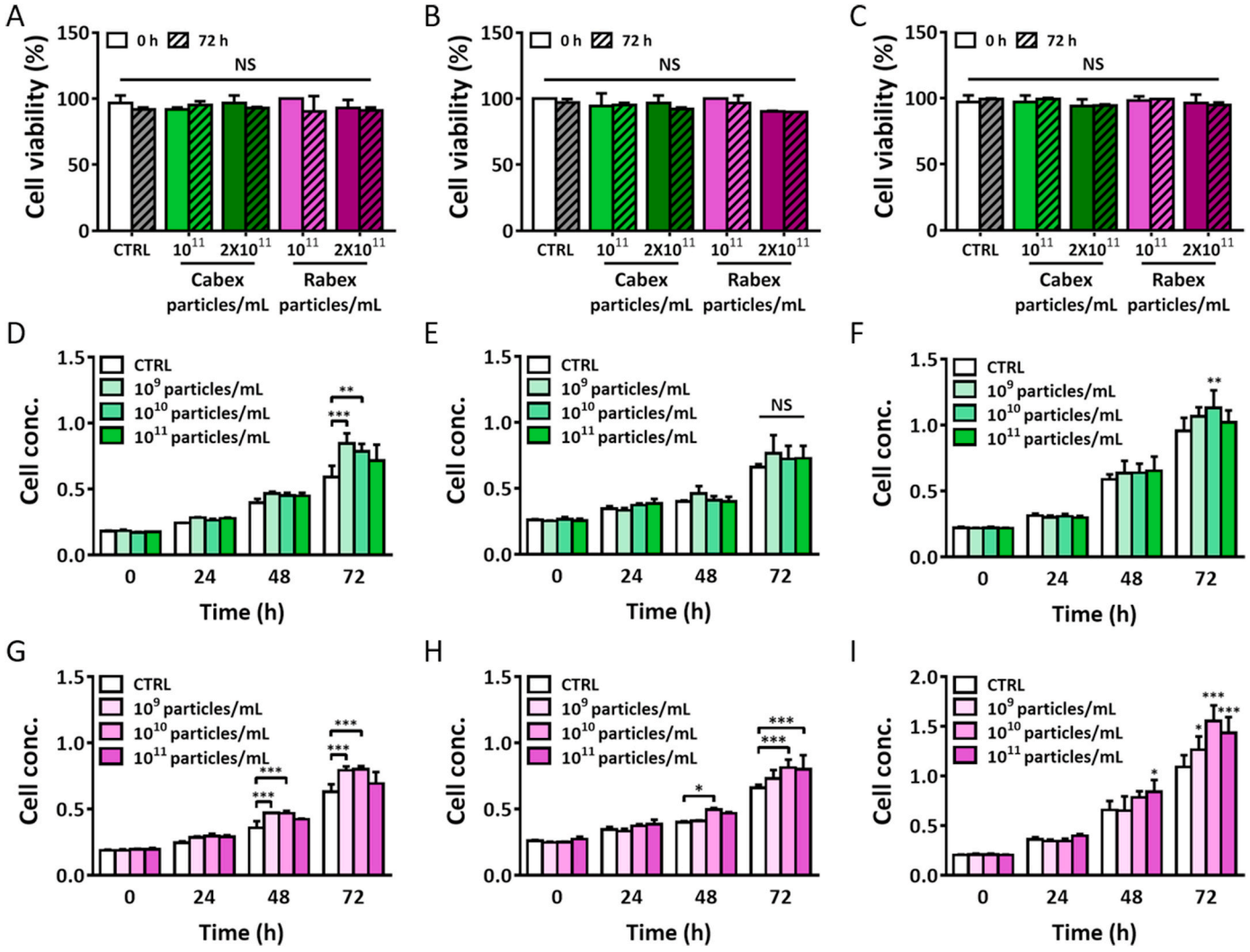

Fig. 4. Cytotoxicity of Cabex and Rabex and their effects on cell proliferation in human cells and murine macrophages. (A–C) Cytotoxicity of Cabex and Rabex. (A) HaCaT, (B) HDF, and (C) RAW264.7 cells were supplemented with Cabex or Rabex, and cell viability was measured at 0 and 72 h. Note that no cytotoxicity was observed for either nanovesicle type in all cells. (D–F) Time- and dose-dependent effects of Cabex on cell proliferation. (D) HaCaT, (E) HDF, and (F) RAW264.7 cells were supplemented with different concentrations of Cabex, and cell concentrations were measured at 0, 24, 48, and 72 h using a WST-1 assay. (G–I) Time- and dose-dependent effects of Rabex on cell proliferation. (G) HaCaT, (H) HDF, and (I) RAW264.7 cells were supplemented with different concentrations of Rabex, and cell concentrations were measured at 0, 24, 48, and 72 h. All values are expressed as mean ± SD (*$p < 0.05$, **$p < 0.01$, ***$p < 0.001$, NS: not significant; $n = 3$).

2.4. Inhibition of inflammation by Cabex and Rabex

Although there have not been many studies investigating the biological functions of plant-derived nanovesicles, a number of studies have reported the anti-inflammatory activities of components extracted from plants using organic solvents [44–46]. To investigate the anti-inflammatory activities of Cabex and Rabex, RAW264.7 cells were supplemented with 0, 1×10^8, 1×10^9, 1×10^{10}, and 1×10^{11} particles mL^{-1} of nanovesicles and treated with LPS to induce inflammation [47, 48]. Proinflammatory transcripts, including IL-6, IL-1β, and COX-2 [49–52], were analyzed by RT-PCR. As shown in Fig. 5A, a 20, 591-fold increase in IL-6 mRNA was observed when cells were treated with LPS in the absence of nanovesicle supplementation. However, IL-6 mRNA levels drastically decreased in a dose-dependent manner with Cabex supplementation, and an only 134.3-fold increase was observed after LPS treatment when 1×10^{11} particles/mL of Cabex had been added. The expression of IL-1β was also effectively suppressed as the concentration of Cabex increased (Fig. 5B). COX-2, another key regulator of inflammation, was also significantly downregulated by Cabex supplementation prior to LPS treatment (Fig. 5C). COX-2 levels increased 1398-fold upon LPS treatment without Cabex compared to 272.8-fold when cells were supplemented with 1×10^{11} particles mL^{-1} of Cabex. The suppressive effects of Rabex on IL-6, IL-1β, and COX-2 expression were also assessed. Rabex also suppressed the expression of IL-6 and IL-1β after LPS treatment (Fig. 5D and E). However, there was no significant difference in COX-2 mRNA levels after Rabex supplementation (Fig. 5F).

The effect of Cabex and Rabex on proinflammatory protein expression was further analyzed. Cytokine levels of IL-6 and IL-1β after LPS treatment were assessed by ELISA (Fig. 5G and H). IL-6 levels decreased to 42.1% and 36.4% after Cabex and Rabex supplementation, respectively, as compared to LPS-treated cells without nanovesicle supplementation. IL-1β levels also decreased to 46.2% and 50.3% after Cabex and Rabex supplementation, respectively. COX-2 protein expression was analyzed by Western blot (Fig. 5I and J). COX-2 levels increased after LPS treatment. However, the LPS-induced increases were significantly suppressed to 45.3% and 58.2% through Cabex and Rabex supplementation, respectively. While the RT-PCR results indicated that Rabex did not affect COX-2 mRNA levels, Rabex downregulated COX-2 protein levels. Based on this, Rabex may regulate the post-transcriptional events during COX-2 expression in cells treated with LPS. Overall, both Cabex and Rabex had clear anti-inflammatory activities and successfully suppressed proinflammatory molecule production in cells.

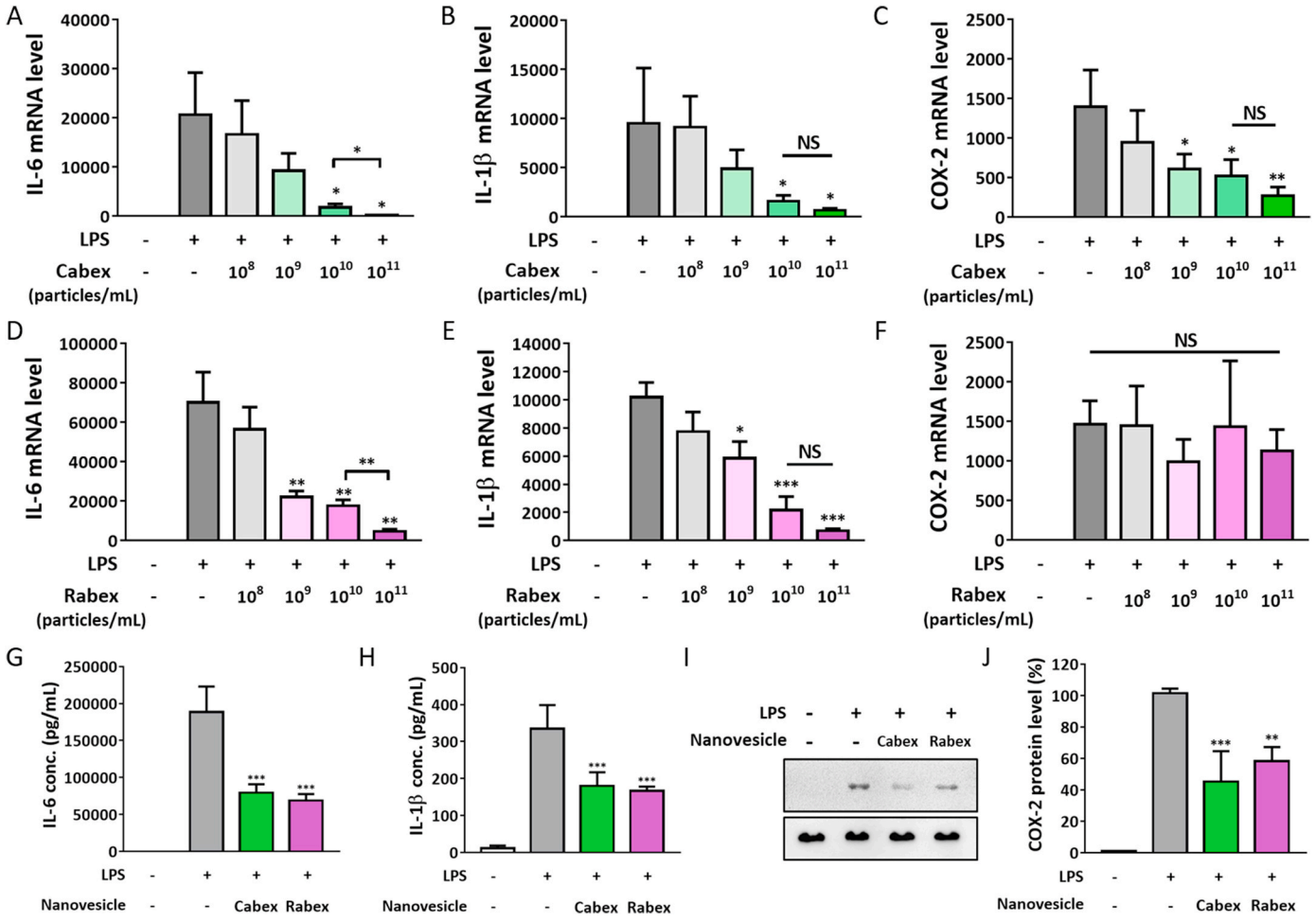

Fig. 5. Anti-inflammatory effects of Cabex and Rabex in LPS-treated RAW264.7 cells. (A–C) Dose-response curves of Cabex on (A) IL-6, (B) IL-1β, and (C) COX-2 mRNA expression levels analyzed by RT-PCR. Cells were supplemented with different concentrations of Cabex followed by inflammation induction by LPS treatment. (D–F) Dose-response curves of Rabex on (D) IL-6, (E) IL-1β, and (F) COX-2 mRNA expression levels analyzed by RT-PCR. Cells were supplemented with different concentrations of Rabex followed by inflammation induction by LPS treatment. (G–H) The effect of Cabex and Rabex on (G) IL-6 and (H) IL-1β protein secretion in LPS-treated cells analyzed by ELISA (I) Western blot analysis of COX-2 protein levels in LPS-treated cells in the absence and presence of Cabex or Rabex. (J) Quantitative analysis of COX-2 protein expression based on Western blot results. The band intensity was quantified by normalization to GAPDH protein levels. All values are expressed as mean ± SD (*$p < 0.05$, **$p < 0.01$, ***$p < 0.001$, NS: not significant; $n = 3$).

2.5. Inhibition of apoptosis by Cabex and Rabex

Aberrant apoptosis contributes to diseases, including Parkinson's or Alzheimer's [53,54]. Moreover, strategies for the production of anti-apoptotic biopharmaceutical drugs using mammalian cell cultures can be of great benefit to patients [55,56]. In this context, we investigated the effect of Cabex and Rabex on apoptosis in HaCaT cells and HDFs. To assess the anti-apoptotic effects of Cabex and Rabex, cells were cultured in the absence or presence of Cabex or Rabex followed by staurosporine (STS) treatment for apoptosis induction. As shown in Fig. 6A, HaCaT cell viability dropped to 30.6% 18 h after STS treatment when cells were cultured without nanovesicle supplementation. In contrast, the decrease in viability after STS treatment was significantly inhibited by nanovesicle supplementation. Cell viability of 55.3% and 65.6% was observed when cells were supplemented with Cabex and Rabex, respectively, 18 h after STS treatment. As the same nanovesicle concentration (1×10^{11} particles mL^{-1}) was used for apoptosis inhibition, Rabex exhibited stronger apoptosis inhibition capacity in HaCaT

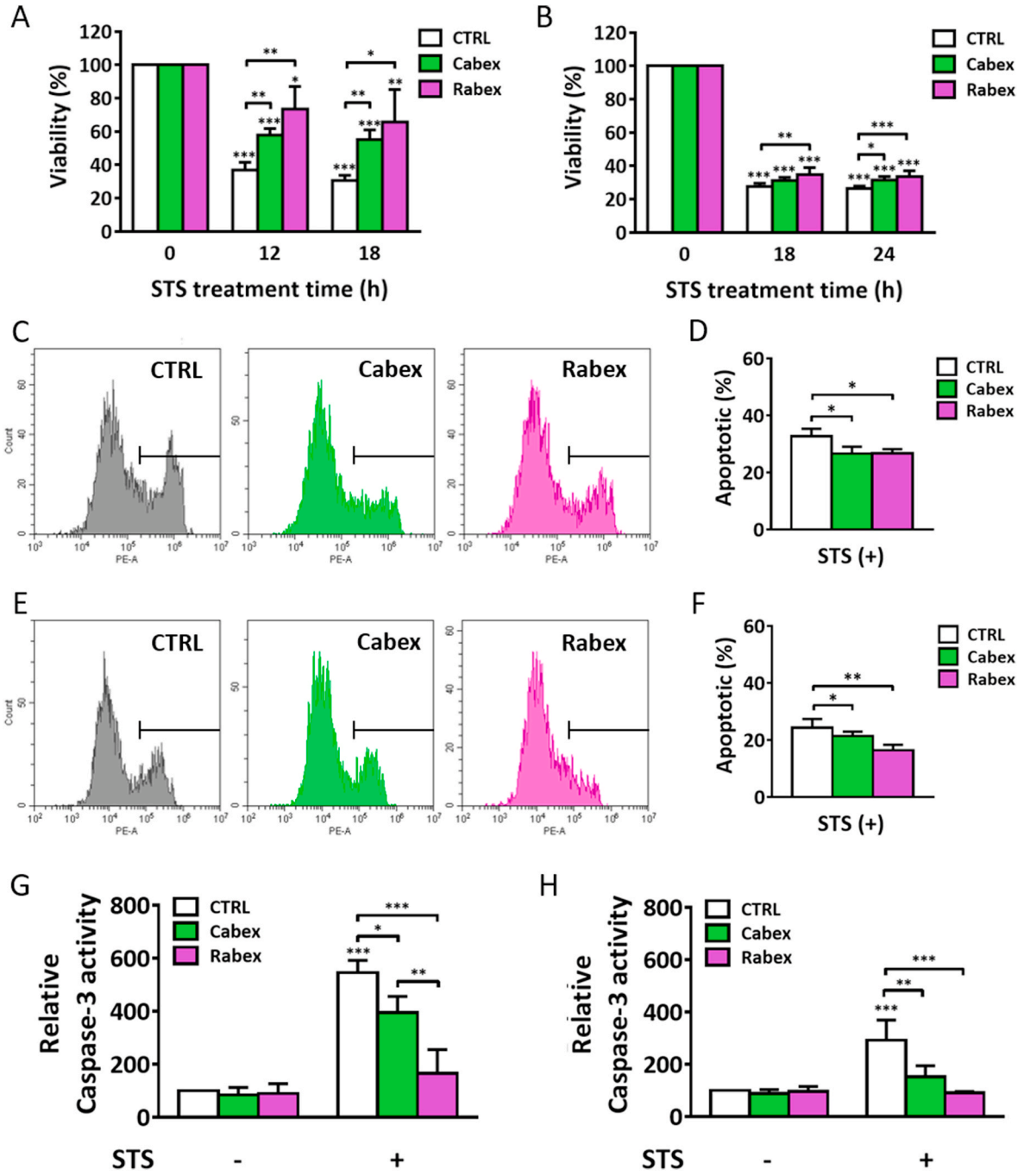

Fig. 6. Anti-apoptotic effect of Cabex and Rabex in human cells. (A, B) Cells were supplemented with 1×10^{11} particles mL^{-1} of Cabex or Rabex followed by apoptosis induction using STS. Cell viability was measured by a WST-1 assay in (A) HaCaT cells and (B) HDFs. (C) Flow cytometric analysis of HaCaT cell viability after STS treatment in the absence or presence of Cabex or Rabex. (D) Percentages of apoptotic cells of STS-treated HaCaT cells based on the flow cytometric analysis in (C). (E) Flow cytometric analysis of HDF viability after STS treatment in the absence or presence of Cabex or Rabex. (F) Percentages of apoptotic cells of STS-treated HDF based on the flow cytometric analysis in (E). (G, H) Inhibition of caspase-3 activity in (G) HaCaT cells and (H) HDFs by Cabex and Rabex. All values are expressed as mean ± SD (*$p < 0.05$, **$p < 0.01$, ***$p < 0.001$; $n = 3$).

cells. Both Cabex and Rabex exhibited an anti-apoptotic effect in HDFs (Fig. 6B), indicating that the decrease in cell viability was effectively suppressed by nanovesicles. We further assessed the viability of cells after STS treatment by flow cytometry to clearly demonstrate the anti-apoptotic effects of Cabex and Rabex. After nanovesicle supplementation, HaCaT cells and HDFs were treated with STS for 6 h and 24 h, respectively (Fig. 6C–F). Flow cytometric results clearly demonstrated that Cabex and Rabex reduced the percentage of apoptotic cells after apoptosis induction.

We further investigated the effect of plant-derived nanovesicles on caspase-3 activation, which is a key event in apoptosis [57,58]. HaCaT cells and HDFs were cultured in the absence or presence of nanovesicles followed by STS treatment, and caspase-3 activity was measured in cell lysates (Fig. 6G and H). In HaCaT cells, caspase-3 activity drastically increased to 546% after STS treatment. However, the activation of caspase-3 was significantly suppressed by Cabex as it only increased up

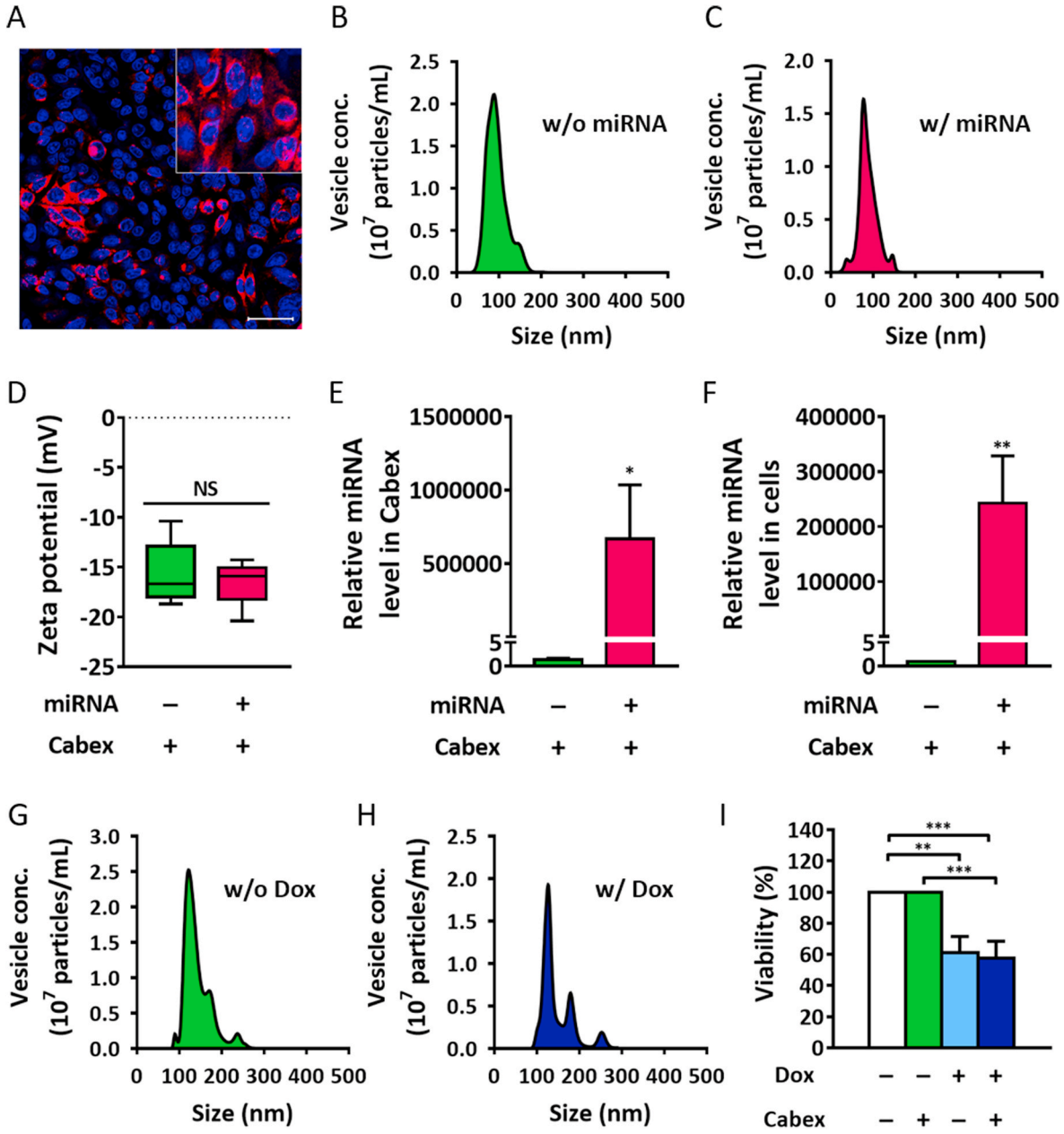

Fig. 7. Investigation of Cabex as therapeutic drug delivery vehicles. (A) Fluorescence microscopy showing the delivery of DNA oligonucleotides (red) by Cabex. Fluorescence-labeled DNA oligonucleotides were loaded into Cabex, and cells were then incubated with drug-loaded Cabex for delivery. Hoechst 33342 was used for nuclei staining (Blue). Scale bar indicates 50 μm. (B–F) Analysis of miRNA loading into Cabex and intracellular delivery of miRNA. (B, C) EV size distribution profiles (B) without and (C) with miRNA loading into Cabex. (D) Comparison of zeta potential of Cabex without and with miRNA loading. No significant difference was observed. (E) RT-PCR analysis of miRNA in Cabex. miRNA was loaded into Cabex, and the relative amount of loaded miRNA was assessed. The relative miRNA level in Cabex indicates the amount of miR-184 in Cabex with miR-184 was normalized by that in Cabex without miR-184. (F) Delivery of miRNA to SW480 cells by Cabex. Intracellular miRNA levels before and after miRNA delivery by Cabex were measured using RT-PCR. The relative miRNA level in cells supplemented with Cabex with miR-184 was normalized by Cabex without miR-184. (G, H) Size distribution of Cabex (G) without and (H) with a chemotherapeutic (doxorubicin) drug load. (I) Anti-cancer effect of Cabex loaded with doxorubicin. SW480 cells were treated with Cabex, doxorubicin, and doxorubicin-loaded Cabex for 72 h, and cell viability was measured by a WST-1 assay. All values are expressed as mean ± SD (*p < 0.05, **p < 0.01, ***p < 0.001, NS: not significant; $n = 3$). (For interpretation of the references to color in this figure legend, the reader is referred to the Web version of this article.)

to 395%. Caspase-3 activity was further suppressed by the same concentration of Rabex, resulting in an activity of 166%. Similar anti-apoptotic patterns were observed in STS-treated HDFs (Fig. 6H). This indicates that Cabex and Rabex contain anti-apoptotic components that can suppress apoptosis and protect cells from stress. Rabex induced greater resistance to apoptosis than Cabex, indicating that Rabex may contain a higher concentration of molecules that regulate apoptosis. These results support the potential of plant-derived nanovesicles in the treatment of diseases related to aberrant apoptosis.

2.6. Cabex and Rabex as novel therapeutic drug delivery vehicles

There has been extensive research on the development of drug delivery vehicles utilizing EVs produced by various types of mammalian cells [13,14,59]. Compared to artificially synthesized carriers, EVs are biocompatible nanoparticles with minimal cytotoxicity when used *in vivo* [60]. In addition, the lipid bilayer of EVs comprises a protective barrier around encapsulated cargo, especially important for miRNAs, since RNA-based drugs are unstable [61]. However, there is a critical issue with using mammalian cell-derived EVs, including exosomes, as therapeutic drug delivery carriers. Unlike *in vitro* cellular studies and *in vivo* animal studies in mice or rats, the clinical application of EVs in humans requires a huge number of EVs to be injected [62]. As mentioned earlier, since mammalian cell-derived EVs are normally obtained through cell culture, large-scale EV production requires a scale-up that is cost- and time-effective. In addition, mammalian cell cultures require the use of animal components, including FBS, which can cause critical safety problems in clinical applications [63]. Thus, plant-derived nanovesicles offer great advantages over mammalian cell culture-derived EVs and synthetic nanoparticles. For instance, the average yield of Cabex was 1.504×10^{11} particles g^{-1} cabbage (Fig. S2D). The average retail price of cabbage reported by the United States Department of Agriculture (USDA) is only \$0.00137 g^{-1}. As the wholesale price of cabbages is even lower than the retail price, the use of Cabex would be very cost-effective in addition to its functional advantages over cell culture-derived EVs.

2.7. Nucleic acid-based drug delivery by Cabex

In order to demonstrate that plant-derived nanovesicles can be used as drug delivery vehicles, we loaded fluorescent dye-labeled anti-sense DNA oligonucleotides to Cabex followed by DNA oligonucleotide-containing Cabex delivery to cells (Fig. 7A). After 6 h of incubation with Cabex, strong fluorescent signals were observed, especially in the cytosol, indicating that Cabex successfully delivered anti-sense DNA oligonucleotides to human cells. We then used miRNA as a nucleic acid drug candidate and loaded it into Cabex. It was previously discovered that the presence of large amounts of small RNAs, especially miRNAs, in EVs [64]. It was also found that EV-mediated transfer of RNAs is a novel mechanism of genetic exchange among cells. Since then, there have been extensive studies using EVs as delivery vehicles of miRNAs for cancer therapy. miRNAs have advantage over mRNAs for the encapsulation into EVs because of their small size. Also, in general, miRNAs have multiple mRNA targets and the inhibition of their functions contributes to the development of many diseases including cancer [65–67]. miR-184 was chosen as a representative miRNA drug because it is involved in a wide range of biological and pathological processes, including proliferation, apoptosis, and oncogenesis [68,69]. After loading, undelivered free miRNAs were removed using ultrafiltration. As shown in Fig. 7B and C, there was no difference in the size and distribution of Cabex before and after miRNA loading, indicating that loading did not cause morphological changes in Cabex. There was no significant difference in the zeta potential of Cabex regardless of miRNA loading, probably because loaded miRNAs are encapsulated inside the Cabex (Fig. 7D). We also measured the relative amount of encapsulated miRNA in exosomes by real-time PCR (Fig. 7E). There was a 667,000-fold increase in miRNA levels after miRNA loading into Cabex, indicative of a high number of miRNAs loaded. The relative amount of miRNA delivered to cells by Cabex was also assessed (Fig. 7F). miRNA-loaded Cabex were administered to colon cancer cells for 72 h, and the levels of miRNA before and after delivery were measured by real-time PCR. A more than 246,000-fold increase in miRNA was observed in cells treated with Cabex.

2.8. Anti-cancer chemotherapeutic drug delivery by Rabex

As there have been no extensive studies on the delivery of anti-cancer chemotherapeutic drugs using cell-derived EVs, we investigated whether plant-derived nanovesicles could deliver chemotherapeutics to human cells. Cabex was incubated with a representative anti-cancer drug, doxorubicin, in order to encapsulate the drug into vesicles. Unloaded free doxorubicin was removed by ultrafiltration. NTA analysis revealed similar size distributions regardless of doxorubicin loading (Fig. 7G and H). SW480 colon cancer cells were then incubated with doxorubicin-loaded Cabex, and cell concentration was assessed. The same concentrations of doxorubicin (1 μM) or Cabex (1×10^9 particles mL^{-1}) alone were also tested as controls. Doxorubicin-loaded Cabex effectively suppressed colon cancer cell proliferation, and cell viability was drastically reduced to 61.0 and 57.5% after treatment with doxorubicin alone and doxorubicin-loaded Cabex, respectively (Fig. 7I). This indicated that doxorubicin was loaded onto Cabex and successfully delivered to cancer cells, where it entered the nucleus to exert its cytotoxic effects. To verify Rabex can be also used for chemotherapeutic drug delivery, the same experiments were performed by constructing doxorubicin-loaded Rabex (Fig. S3). Similar size distribution was observed between Rabex and drug-loaded Rabex (Figs. S3A and B). Also, doxorubicin-loaded Rabex further suppressed cell growth that the viability was reduced to 39.5 and 32.4% after treatment with doxorubicin alone and doxorubicin-loaded Rabex, respectively (Fig. S3C). Plant-derived nanovesicles, including Cabex and Rabex, can substitute cell culture-produced EVs and be used as novel delivery vehicles for different types of drugs. As high concentrations of nanovesicles with high purity can be efficiently isolated from cabbage using our method, Cabex and Rabex have therapeutic potential owing to multiple biological functions, including cell proliferation promotion, inflammation and apoptosis inhibition, and efficient drug delivery to cells.

Further studies exploring the molecular mechanism of Cabex or Rabex regarding the promoting proliferation and inhibiting apoptosis and inflammation are essential because it is possible that those events are closely related at the molecular levels. For instance, the activation of Janus kinase 2 (JAK2)/STAT3 signaling pathway which is known to mediate an inflammation response in cells induces the expression of pro-inflammatory genes, including IL-6 and TNF-α. This accelerates the activation of caspase-3 that subsequently induces apoptosis [70–73]. Also, it is reported that many genes that enhance cell proliferation and apoptosis inhibition, including cyclin D, Bcl-2, survivin, Bcl-xL, XIAP (X-linked inhibitor of apoptosis protein), are regulated by JAK2/STAT3 activation [74–76]. That is, the inhibition of JAK2/STAT3 can inhibit both inflammation and apoptosis while promoting cell proliferation. Thus, Cabex and Rabex may contain the molecules that participate and regulate the signaling pathway, including JAK2/STAT3 pathway. Further analysis of the active components responsible for the biological activities of Cabex and Rabex may contribute to a better understanding of their function and broaden their application as therapeutics in humans. There are several potential *in vivo* applications that can be investigated to develop cabbage-derived exosome-like vesicles as novel bioactive materials. Of them, acute colitis model using dextran sulfate sodium (DSS) is particularly useful for the *in vivo* investigation of Cabex and Rabex because Cabex and Rabex significantly suppressed inflammation [77–79]. DDS-induced colitis model is widely used because of its simplicity and similarities with ulcerative colitis in human. Also, for *in vivo* application of Cabex and Rabex as drug delivery vehicles, mouse xenograft tumor model using SW480 colon cancer cell line can be

constructed to evaluate the therapeutic efficacy. Cabex and Rabex can be further engineered and functionalized for their surfaces to enhance the cancer-specificity of anti-cancer drugs. Because Cabex and Rabex have multiple functions, there are many potential applications to be explored to increase the value of these bioactive materials.

3. Conclusion

The current study describes an effective method for exosome-like nanovesicle isolation from cabbage, resulting in a high yield of nanovesicles with high purity. Further, the regulation of cellular functions by Cabex and Rabex was investigated. Cabex and Rabex promoted cell proliferation and significantly inhibited inflammation and apoptosis. Assessment of these plant-derived nanovesicles as drug delivery vehicles demonstrated that high concentrations of therapeutic drugs were successfully encapsulated in Cabex and Rabex and then efficiently delivered to human cells. Considering their low cytotoxicity, multiple functions, low production cost, and high production yield, Cabex and Rabex are novel candidates for therapeutic drug development. In this context, the current results will contribute to a paradigm shift in functional drug development using nanovesicles from plants.

4. Materials and methods

Materials and cell culture: Human keratinocyte (HaCaT), human dermal fibroblast (HDF), and murine macrophage (RAW264.7) cells were cultured in Dulbecco's Modified Eagle's Medium (Corning, USA), supplemented with 10% (v/v) fetal bovine serum (FBS, Gibco, USA), and 1% (v/v) penicillin and streptomycin (Gibco, USA). All cell lines were incubated in a humidified atmosphere of 5% CO_2 at 37 °C. Inflammation was induced by lipopolysaccharide (LPS; Sigma, USA). Apoptosis was induced by incubating cells with STS (Santa Cruz Biotechnology, USA).

Isolation of extracellular vesicles from cabbage and red cabbage: The two types of cabbage used for exosome-like nanovesicle isolation, green cabbage (*Brassica oleracea* var. *capitata* L.) and red cabbage (*Brassica oleracea* var. *capitata* F. *rubra*), were produced by local farms in Korea. Cabbage and red cabbage were washed three times with distilled water to remove dust, soil, and pesticides. The juice was extracted using a blender followed by serial centrifugation at 8000 and 20,000×*g* for 1 h each to remove large debris. The supernatant was stored at −80 °C before isolation. For polyethylene glycol (PEG)-based precipitation, the PEG-containing solution was mixed with plant juice at a 1:5 vol ratio (v/v), and the mixture was incubated at 4 °C overnight. The mixture was then centrifuged at 1500×*g* for 30 min at 4 °C. Supernatant was discarded, and the pellet containing exosome-like nanovesicles was resuspended. For ultracentrifugation, nanovesicles were isolated using an ultracentrifuge (Beckman Coulter, Optima TL, USA) at 120,000×*g* for 2 h. The supernatant was removed, and the pellet containing vesicles was resuspended. The Amicon Ultra-15 centrifugal filter unit was used to concentrate juices followed by exosome-like nanovesicle isolation using size-exclusion chromatography (Izon Science, New Zealand). The fractions were eluted with PBS, and each fraction was assessed for its vesicle and protein concentration. All products used during isolation from cabbage and red cabbage are shown in Fig. S2.

Nanoparticle tracking analysis (NTA), transmission electron microscopy (TEM), and zeta potential analysis: The size distribution and concentration of Cabex and Rabex were analyzed using Nanosight NS300 (Malvern, UK). The same camera level, threshold, and focus were used for all measurements. For TEM, vesicles were absorbed onto a formvar carbon-coated grid for 10 min. After washing the grid with distilled water, Cabex and Rabex were fixed with 2% paraformaldehyde and washed twice with PBS, respectively. The grids were then negatively stained with 2% uranyl acetate for 10 min. Samples were dried for 15 min and visualized using a JEM-1010 electron microscope (JEOL, Japan). The zeta potential of nanovesicles was assessed using Zetasizer Nano ZS (Malvern, UK).

Confocal microscopy of Cabex and Rabex uptake into cells: To verify that plant-derived nanovesicles can be taken up by human cells, Cabex and Rabex were stained with PKH67 green dye (Sigma-Aldrich, USA) followed by incubation with cells. Cabex or Rabex was incubated with PKH67 dye for 15 min at 25 °C, and the mixture was filtrated by ultrafiltration with a 100-kDa filter to remove free PKH67 dye. HaCaT cells were seeded and cultured in medium with PKH67-labeled Cabex or Rabex at a concentration of 1×10^{11} particles mL^{-1} [55,80]. After incubation, Hoechst 33342 fluorescent dye was added to the culture medium for nuclear staining. Cells were washed several times, and intracellular uptake of Cabex or Rabex was analyzed using a confocal laser scanning microscope (Zeiss, Germany).

Effect of Cabex and Rabex on viability and proliferation: To measure cell viability and concentration, cells were seeded in 24-well plates at a density of 1×10^4 cells cm^{-2} and incubated for 24 h. After washing, cells were incubated with EV-free FBS-containing media in the presence or absence of Cabex or Rabex at concentrations ranging from 1.0×10^9 to 1.0×10^{11} particles mL^{-1} for 24 h. Cell viability was measured by staining cells with trypan blue dye, and cell proliferation was measured by a WST-1 assay. For flow cytometric analysis, cells were cultured in medium with or without nanovesicles at a concentration of 1.0×10^{11} particles mL^{-1}. After 24 h, cells were treated with STS, washed twice with PBS, and treated with propidium iodide for 15 min. The proportion of apoptotic cells was measured using a flow cytometer (Beckman Coulter, Inc., USA).

Caspase-3 activity measurement: Cysteinyl aspartic acid protease-3 (caspase-3) activity was measured in STS-treated HaCaT and HDF cells. The cells were harvested, washed twice with cold PBS, and lysed with RIPA buffer (ELPIS-Biotech, Korea). Protein quantification was performed using a bicinchoninic acid (BCA) assay. Cell lysates were incubated with reaction buffer containing Ac-DEVD-AFC (Enzo, USA). Caspase-3 activity was assessed by measuring the fluorescence intensity using a Varioskan™ Flash Multimode Reader (Thermo Scientific, USA) at emission and excitation wavelengths of 400 and 505 nm, respectively.

Real-time polymerase chain reaction analysis of inflammatory gene expression and enzyme-linked immunosorbent assay cytokine detection: To assess the effect of Cabex and Rabex on inflammation-related gene expression, real-time polymerase chain reaction (RT-PCR) was performed using the StepOnePlus Real-Time PCR System (Applied Biosystems, USA). RAW264.7 cells were cultured in the presence or absence of EVs, followed by induction of inflammation by LPS. RNA was isolated using the RNeasy Mini Kit (Qiagen, Germany) according to the manufacturer's protocol, and RNA concentration was determined using a microplate reader (BioTek Instruments, USA). cDNA was synthesized using ReverTra Ace qPCR RT Master Mix (Toyobo, Japan), and RT-PCR was performed using the THUNDERBIRD SYBR qPCR mix (Toyobo, Japan).

To analyze proinflammatory cytokine secretion, RAW264.7 cells were cultured in the presence or absence of nanovesicles, followed by inflammation induction via LPS. Cell culture medium containing secreted cytokines was collected and stored before analysis using an ELISA kit (R&D system, USA) following the manufacturer's protocol. Absorbance was measured using a Varioskan™ Flash Multimode Reader (Thermo Scientific, USA) at 450 nm.

Western blot analysis: RAW264.7 cells were supplemented with Cabex or Rabex and treated with LPS for induction of inflammation. Cells were lysed in RIPA buffer, and protein concentration was determined by BCA assay. 20 μg of protein was separated by SDS-PAGE under reducing conditions. Separated proteins were then transferred to a PVDF membrane in Towbin transfer buffer at 80 V for 2 h. Membranes were blocked with 5% skim milk and were then incubated with a COX-2 antibody (Abcam, UK) or a GAPDH antibody (Cell Signaling Technology, USA) overnight at 4 °C. An anti-rabbit IgG antibody conjugated to horseradish peroxidase (HRP) (Cell Signaling Technology, USA) was used as the secondary antibody. ECL Prime Western Blotting Detection Reagent (GE Healthcare, UK) was used for the chemiluminescence reaction, and

Western blot results were analyzed using ChemiDoc™ XRS + System (Bio-Rad, USA).

Drug loading and delivery by Cabex and Rabex: To demonstrate that plant-derived nanovesicles can be used as drug delivery vehicles, First, miRNAs were loaded onto Cabex and then delivered to SW480 cells. miR-184 (Thermo Fisher Scientific, USA) was used as a model miRNA drug. To generate miRNA-loaded Cabex, Cabex was transfected with miR-184 using the Lipofectamine RNAiMAX Reagent kit (Thermo Fisher Scientific, USA) according to the manufacturer's instructions. Briefly, 200 pmol of miR-184 was mixed with the reagent and further incubated with 1×10^{11} Cabex particles for 6 h at 37 °C. Unloaded free miRNAs were removed by ultrafiltration with a 100-kDa filter (Merck Millipore, USA). To test the delivery of an anti-cancer chemotherapeutic, 100 μM of doxorubicin (LC Laboratories, USA) was incubated with 1×10^{11} particles of Rabex for 4 h at 37 °C. Unloaded free doxorubicin was removed by ultrafiltration. The amount of loaded doxorubicin was assessed by measuring fluorescence intensity (excitation: 470 nm, emission: 595 nm).

Statistical analysis: Results are expressed as mean ± standard deviation (SD), $n \geq 3$. Data were analyzed using one-way and two-way ANOVA, and $p < 0.05$ was considered statistically significant. All statistical analyses obtained from independent experiments were performed using the GraphPad Prism 7.0 software (GraphPad, USA).

Declaration of competing interest

The authors declare that they have no known competing financial interests or personal relationships that could have appeared to influence the work reported in this paper.

CRediT authorship contribution statement

Jae Young You: Investigation, Formal analysis, Writing – original draft. **Su Jin Kang:** Investigation, Formal analysis, Validation, Writing – original draft, revision, Writing – review & editingediting. **Won Jong Rhee:** Conceptualization, Validation, Resources, Funding acquisition, Writing – review & editingWriting – review, revision, & editing.

Acknowledgements

This work was supported by a National Research Foundation of Korea (NRF) grant funded by the Korean Government (MSIT) (NRF-2016R1A5A1010148, NRF-2019R1A2C1003111).

Appendix A. Supplementary data

Supplementary data to this article can be found online at https://doi.org/10.1016/j.bioactmat.2021.04.023.

References

[1] J.C. Akers, D. Gonda, R. Kim, B.S. Carter, C.C. Chen, Biogenesis of extracellular vesicles (EV): exosomes, microvesicles, retrovirus-like vesicles, and apoptotic bodies, J. Neuro Oncol. 113 (2013) 1–11.
[2] A.A. Patil, W.J. Rhee, Exosomes: biogenesis, composition, functions, and their role in pre-metastatic niche formation, Biotechnol. Bioproc. Eng. 24 (2019) 689–701.
[3] G. Raposo, W. Stoorvogel, Extracellular vesicles: exosomes, microvesicles, and friends, J. Cell Biol. 200 (2013) 373–383.
[4] A.H. Mirza, S. Kaur, L.B. Nielsen, J. Størling, R. Yarani, M. Roursgaard, et al., Breast milk-derived extracellular vesicles enriched in exosomes from mothers with type 1 diabetes contain aberrant levels of microRNAs, Front. Immunol. 10 (2019) 2543.
[5] M.-P. Caby, D. Lankar, C. Vincendeau-Scherrer, G. Raposo, C. Bonnerot, Exosomal-like vesicles are present in human blood plasma, Int. Immunol. 17 (2005) 879–887.
[6] Y. Ogawa, Y. Miura, A. Harazono, M. Kanai-Azuma, Y. Akimoto, H. Kawakami, et al., Proteomic analysis of two types of exosomes in human whole saliva, Biol. Pharm. Bull. 34 (2011) 13–23.
[7] P. Penfornis, K.C. Vallabhaneni, J. Whitt, R. Pochampally, Extracellular vesicles as carriers of microRNA, proteins and lipids in tumor microenvironment, Int. J. cancer. 138 (2016) 14–21.
[8] A. Becker, B.K. Thakur, J.M. Weiss, H.S. Kim, H. Peinado, D. Lyden, Extracellular vesicles in cancer: cell-to-cell mediators of metastasis, Canc. Cell 30 (2016) 836–848.
[9] Y.G. Kim, U. Park, B.J. Park, K. Kim, Exosome-mediated bidirectional signaling between mesenchymal stem cells and chondrocytes for enhanced chondrogenesis, Biotechnol. Bioproc. Eng. 24 (2019) 734–744.
[10] S. El Andaloussi, I. Mäger, X.O. Breakefield, M.J.A. Wood, Extracellular vesicles: biology and emerging therapeutic opportunities, Nat. Rev. Drug Discov. 12 (2013) 347–357.
[11] S. Samanta, S. Balasubramanian, S. Rajasingh, U. Patel, A. Dhanasekaran, B. Dawn, et al., MicroRNA: a new therapeutic strategy for cardiovascular diseases, Trends Cardiovasc. Med. 26 (2016) 407–419.
[12] C. Grange, S. Tritta, M. Tapparo, M. Cedrino, C. Tetta, G. Camussi, et al., Stem cell-derived extracellular vesicles inhibit and revert fibrosis progression in a mouse model of diabetic nephropathy, Sci. Rep. 9 (2019) 4468.
[13] K. Jeong, S. Jeong, J.A. Kim, W.J. Rhee, Exosome-based antisense locked nucleic acid delivery for inhibition of type II collagen degradation in chondrocyte, J. Ind. Eng. Chem. 74 (2019) 126–135.
[14] K. Jeong, Y.J. Yu, J.Y. You, W.J. Rhee, J.A. Kim, Exosome-mediated microRNA-497 delivery for anti-cancer therapy in a microfluidic 3D lung cancer model, Lab Chip 20 (2020) 548–557.
[15] J. Mu, X. Zhuang, Q. Wang, H. Jiang, Z.B. Deng, B. Wang, et al., Interspecies communication between plant and mouse gut host cells through edible plant derived exosome-like nanoparticles, Mol. Nutr. Food Res. 58 (2014) 1561–1573.
[16] M. Zhang, E. Viennois, C. Xu, D. Merlin, Plant derived edible nanoparticles as a new therapeutic approach against diseases, Tissue Barriers 4 (2016), e1134415.
[17] S. Ju, J. Mu, T. Dokland, X. Zhuang, Q. Wang, H. Jiang, et al., Grape exosome-like nanoparticles induce intestinal stem cells and protect mice from DSS-induced colitis, Mol. Ther. 21 (2013) 1345–1357.
[18] M. Zhang, E. Viennois, M. Prasad, Y. Zhang, L. Wang, Z. Zhang, et al., Edible ginger-derived nanoparticles: a novel therapeutic approach for the prevention and treatment of inflammatory bowel disease and colitis-associated cancer, Biomaterials 101 (2016) 321–340.
[19] M. De Robertis, A. Sarra, V. D'Oria, F. Mura, F. Bordi, P. Postorino, et al., Blueberry-derived exosome-like nanoparticles counter the response to TNF-alpha-induced change on gene expression in EA.hy926 cells, Biomolecules 10 (5) (2020) 742.
[20] F. Perut, L. Roncuzzi, S. Avnet, A. Massa, N. Zini, S. Sabbadini, et al., Strawberry-derived exosome-like nanoparticles prevent oxidative stress in human mesenchymal stromal cells, Biomolecules 11 (1) (2021) 87.
[21] A.L.D. Stefania Raimondo, Antonietta Di Bella, Flores Naselli, Laura Saieva, Simona Fontana, Giovanni Zito, Giacomo De Leo, Flugy Anna, Francesca Monteleone, Mauro Manno, Riccardo Alessandro, Citrus limon-derived nanovesicles inhibit cancer cell proliferation and suppress CML xenograft growth by inducing TRAIL-mediated cell death, Oncotarget 6 (2015) 19514–19527.
[22] M. Zhang, B. Xiao, H. Wang, M.K. Han, Z. Zhang, E. Viennois, et al., Edible ginger-derived nano-lipids loaded with doxorubicin as a novel drug-delivery approach for colon cancer therapy, Mol. Ther. 24 (2016) 1783–1796.
[23] C. Yang, M. Zhang, D. Merlin, Advances in plant-derived edible nanoparticle-based lipid nano-drug delivery systems as therapeutic nanomedicines, J. Mater. Chem. B 6 (2018) 1312–1321.
[24] Q. Wang, X. Zhuang, J. Mu, Z.-B. Deng, H. Jiang, L. Zhang, et al., Delivery of therapeutic agents by nanoparticles made of grapefruit-derived lipids, Nat. Commun. 4 (2013) 1867.
[25] W. Halperin, W.A. Jensen, Ultrastructural changes during growth and embryogenesis in carrot cell cultures, J. Ultrastruct. Res. 18 (1967) 428–443.
[26] P. Pérez-Bermúdez, J. Blesa, J.M. Soriano, A. Marcilla, Extracellular vesicles in food: experimental evidence of their secretion in grape fruits, Eur. J. Pharmaceut. Sci. 98 (2017) 40–50.
[27] J. Webber, A. Clayton, How pure are your vesicles? J. Extracell. Vesicles 2 (2013) 19861.
[28] J.Z. Nordin, Y. Lee, P. Vader, I. Mäger, H.J. Johansson, W. Heusermann, et al., Ultrafiltration with size-exclusion liquid chromatography for high yield isolation of extracellular vesicles preserving intact biophysical and functional properties, Nanomedicine 11 (2015) 879–883.
[29] M.I. Ramirez, M.G. Amorim, C. Gadelha, I. Milic, J.A. Welsh, V.M. Freitas, et al., Technical challenges of working with extracellular vesicles, Nanoscale 10 (2018) 881–906.
[30] C.Y. Soo, Y. Song, Y. Zheng, E.C. Campbell, A.C. Riches, F. Gunn-Moore, et al., Nanoparticle tracking analysis monitors microvesicle and exosome secretion from immune cells, Immunology 136 (2012) 192–197.
[31] M. Zhang, X. Wang, M.K. Han, J.F. Collins, D. Merlin, Oral administration of ginger-derived nanolipids loaded with siRNA as a novel approach for efficient siRNA drug delivery to treat ulcerative colitis, Nanomedicine 16 (2018) 1927–1943.
[32] C. Yang, M. Zhang, D. Merlin, Advances in plant-derived edible nanoparticle-based lipid nano-drug delivery systems as therapeutic nanomedicines, J. Mater. Chem. B. 6 (2018) 1312–1321.
[33] Q. Wang, Y. Ren, J. Mu, N.K. Egilmez, X. Zhuang, Z. Deng, et al., Grapefruit-derived nanovectors use an activated leukocyte trafficking pathway to deliver therapeutic agents to inflammatory tumor sites, Canc. Res. 75 (2015) 2520–2529.
[34] M.L. Trevor Glaros, Liwu Li, Macrophages and fibroblasts during inflammation, tissue damage and organ injury, Front. Biosci. 14 (2009) 3988–3993.
[35] J.J. O'Shea, P.J. Murray, Cytokine signaling modules in inflammatory responses, Immunity 28 (2008) 477–487.

[36] J.M. Reinke, H. Sorg, Wound repair and regeneration, Eur. Surg. Res. 49 (2012) 35–43.
[37] T. Fujiwara, S. Kanazawa, R. Ichibori, T. Tanigawa, T. Magome, K. Shingaki, et al., L-arginine stimulates fibroblast proliferation through the GPRC6A-ERK1/2 and PI3K/Akt pathway, PloS One 9 (2014), e92168.
[38] S.W.A.R. Grose, Regulation of wound healing by growth factors and cytokines, Physiol. Rev. 83 (2003) 835–870.
[39] M. Nakanishi-Matsui, S. Yano, N. Matsumoto, M. Futai, Lipopolysaccharide induces multinuclear cell from RAW264.7 line with increased phagocytosis activity, Biochem. Biophys. Res. Commun. 425 (2012) 144–149.
[40] S. Han, H. Gao, S. Chen, Q. Wang, X. Li, L.J. Du, et al., Procyanidin A1 alleviates inflammatory response induced by LPS through NF-kappaB, MAPK, and Nrf2/HO-1 pathways in RAW264.7 cells, Sci. Rep. 9 (2019) 15087.
[41] A. Rhule, S. Navarro, J.R. Smith, D.M. Shepherd, Panax notoginseng attenuates LPS-induced pro-inflammatory mediators in RAW264.7 cells, J. Ethnopharmacol. 106 (2006) 121–128.
[42] I. Elisia, H.B. Pae, V. Lam, R. Cederberg, E. Hofs, G. Krystal, Comparison of RAW264.7, human whole blood and PBMC assays to screen for immunomodulators, J. Immunol. Methods 452 (2018) 26–31.
[43] L.J. Berghaus, J.N. Moore, D.J. Hurley, M.L. Vandenplas, B.P. Fortes, M.A. Wolfert, et al., Innate immune responses of primary murine macrophage-lineage cells and RAW 264.7 cells to ligands of Toll-like receptors 2, 3, and 4, Comp. Immunol. Microbiol. Infect. Dis. 33 (2010) 443–454.
[44] Y. Lee, S. Kim, B. Yang, C. Lim, J.-H. Kim, H. Kim, et al., Anti-inflammatory effects of Brassica oleracea var. Capitata L. (Cabbage) methanol extract in mice with contact dermatitis, Phcog. Mag. 14 (2018) 174–179.
[45] P. Mizgier, A.Z. Kucharska, A. Sokół-Łętowska, J. Kolniak-Ostek, M. Kidoń, I. Fecka, Characterization of phenolic compounds and antioxidant and anti-inflammatory properties of red cabbage and purple carrot extracts, J. Funct. Foods 21 (2016) 133–146.
[46] C.-J.L. Sami Rokayya, Yan Zhao, Ying Li, Chang-Hao Sun, Cabbage (Brassica oleracea L. Var. capitata) phytochemicals with antioxidant and anti-inflammatory potential, Asian Pac. J. Cancer Prev. APJCP 14 (2013) 6657–6662.
[47] M. Molteni, S. Gemma, C. Rossetti, The role of toll-like receptor 4 in infectious and noninfectious inflammation, Mediat. Inflamm. 2016 (2016) 6978936.
[48] N.N. Kuzmich, K.V. Sivak, V.N. Chubarev, Y.B. Porozov, T.N. Savateeva-Lyubimova, F. Peri, TLR4 signaling pathway modulators as potential therapeutics in inflammation and sepsis, Vaccines 5 (4) (2017) 34.
[49] T. Tanaka, M. Narazaki, T. Kishimoto, IL-6 in inflammation, immunity, and disease, CSH Perspect Biol 6 (2014) a016295-a.
[50] K. Ren, R. Torres, Role of interleukin-1beta during pain and inflammation, Brain Res. Rev. 60 (2009) 57–64.
[51] C.S. Williams, M. Mann, R.N. DuBois, The role of cyclooxygenases in inflammation, cancer, and development, Oncogene 18 (1999) 7908–7916.
[52] Y.-R. Na, Y.-N. Yoon, D.-I. Son, S.-H. Seok, Cyclooxygenase-2 inhibition blocks M2 macrophage differentiation and suppresses metastasis in murine breast cancer model, PloS One 8 (2013) e63451-e.
[53] B. Favaloro, N. Allocati, V. Graziano, C. Di Ilio, V. De Laurenzi, Role of apoptosis in disease, Aging (Albany NY) 4 (2012) 330–349.
[54] K. Venderova, D.S. Park, Programmed cell death in Parkinson's disease, CSH Perspect Med 2 (2012) a009365.
[55] S. Han, W.J. Rhee, Inhibition of apoptosis using exosomes in Chinese hamster ovary cell culture, Biotechnol. Bioeng. 115 (2018) 1331–1339.
[56] L. Portt, G. Norman, C. Clapp, M. Greenwood, M.T. Greenwood, Anti-apoptosis and cell survival: a review, Biochim. Biophys. Acta 1813 (2011) 238–259.
[57] A.G. Porter, R.U. Jänicke, Emerging roles of caspase-3 in apoptosis, Cell Death Differ. 6 (1999) 99–104.
[58] D.R. McIlwain, T. Berger, T.W. Mak, Caspase functions in cell death and disease, CSH Perspect Biol 5 (2013) a008656.
[59] X. Luan, K. Sansanaphongpricha, I. Myers, H. Chen, H. Yuan, D. Sun, Engineering exosomes as refined biological nanoplatforms for drug delivery, Acta Pharmacol. Sin. 38 (2017) 754–763.
[60] S. Stremersch, R.E. Vandenbroucke, E. Van Wonterghem, A. Hendrix, S.C. De Smedt, K. Raemdonck, Comparing exosome-like vesicles with liposomes for the functional cellular delivery of small RNAs, J. Contr. Release 232 (2016) 51–61.
[61] A. Akbarzadeh, R. Rezaei-Sadabady, S. Davaran, S.W. Joo, N. Zarghami, Y. Hanifehpour, et al., Liposome: classification, preparation, and applications, Nanoscale Res. Lett. 8 (2013) 102.
[62] F. Villa, R. Quarto, R. Tasso, Extracellular vesicles as natural, safe and efficient drug delivery systems, Pharmaceutics 11 (2019) 557.
[63] C.E. Jochems, J.B. van der Valk, F.R. Stafleu, V. Baumans, The use of fetal bovine serum: ethical or scientific problem? Altern Lab Anim 30 (2002) 219–227.
[64] H. Valadi, K. Ekstrom, A. Bossios, M. Sjostrand, J.J. Lee, J.O. Lotvall, Exosome-mediated transfer of mRNAs and microRNAs is a novel mechanism of genetic exchange between cells, Nat. Cell Biol. 9 (2007) 654–659.
[65] L. Min, S. Zhu, L. Chen, X. Liu, R. Wei, L. Zhao, et al., Evaluation of circulating small extracellular vesicles derived miRNAs as biomarkers of early colon cancer: a comparison with plasma total miRNAs, J. Extracell. Vesicles 8 (2019) 1643670.
[66] L. Yu, B. Sui, W. Fan, L. Lei, L. Zhou, L. Yang, et al., Exosomes derived from osteogenic tumor activate osteoclast differentiation and concurrently inhibit osteogenesis by transferring COL1A1-targeting miRNA-92a-1-5p, J. Extracell. Vesicles 10 (2021), e12056.
[67] T. Bjornetro, K.R. Redalen, S. Meltzer, N.S. Thusyanthan, R. Samiappan, C. Jegerschold, et al., An experimental strategy unveiling exosomal microRNAs 486-5p, 181a-5p and 30d-5p from hypoxic tumour cells as circulating indicators of high-risk rectal cancer, J. Extracell. Vesicles 8 (2019) 1567219.
[68] Y.B. Wang, X.H. Zhao, G. Li, J.H. Zheng, W. Qiu, MicroRNA-184 inhibits proliferation and promotes apoptosis of human colon cancer SW480 and HCT116 cells by downregulating C-MYC and BCL-2, J. Cell. Biochem. 119 (2018) 1702–1715.
[69] X.L. Jiancheng Huang, Hongying Li, Zhenyu Su, Jun Wang, Huijun Zhang, Down-regulation of microRNA-184 contributes to the development of cyanotic congenital heart diseases, Int. J. Clin. Exp. Pathol. 8 (2015) 14221–14227.
[70] Q. Yu, K. Zeng, X. Ma, F. Song, Y. Jiang, P. Tu, et al., Resokaempferol-mediated anti-inflammatory effects on activated macrophages via the inhibition of JAK2/STAT3, NF-kappaB and JNK/p38 MAPK signaling pathways, Int. Immunopharm. 38 (2016) 104–114.
[71] S.O. Cho, J.W. Lim, H. Kim, Red ginseng extract inhibits the expression of MCP-1 and iNOS in Helicobacter pylori-infected gastric epithelial cells by suppressing the activation of NADPH oxidase and Jak2/Stat3, J. Ethnopharmacol. 150 (2013) 761–764.
[72] D. Guo, J.R. Li, Y. Wang, L.S. Lei, C.L. Yu, N.N. Chen, Cyclovirobuxinum D suppresses lipopolysaccharide-induced inflammatory responses in murine macrophages in vitro by blocking JAK-STAT signaling pathway, Acta Pharmacol. Sin. 35 (2014) 770–778.
[73] Z. Liu, L. Gan, Z. Zhou, W. Jin, C. Sun, SOCS3 promotes inflammation and apoptosis via inhibiting JAK2/STAT3 signaling pathway in 3T3-L1 adipocyte, Immunobiology 220 (2015) 947–953.
[74] S. Akhtar, I.W. Achkar, K.S. Siveen, S. Kuttikrishnan, K.S. Prabhu, A.Q. Khan, et al., Sanguinarine induces apoptosis pathway in multiple myeloma cell lines via inhibition of the JaK2/STAT3 signaling, Front. Oncol. 9 (2019) 285.
[75] L.B.M. Ralf Buettner, Richard Jove, Activated STAT signaling in human tumors provides novel molecular targets for therapeutic intervention, Clin. Canc. Res. 8 (2002) 945–954.
[76] Z. Chen, Z.C. Han, STAT3: a critical transcription activator in angiogenesis, Med. Res. Rev. 28 (2008) 185–200.
[77] B. Chassaing, J.D. Aitken, M. Malleshappa, M. Vijay-Kumar, Dextran sulfate sodium (DSS)-induced colitis in mice, Curr. Protoc. Im. 104 (2014) 15.25.1–15.25.14.
[78] J.J. Kim, M.S. Shajib, M.M. Manocha, W.I. Khan, Investigating intestinal inflammation in DSS-induced model of IBD, JoVE 60 (2012) 3678.
[79] W. Shin, H.J. Kim, Intestinal barrier dysfunction orchestrates the onset of inflammatory host-microbiome cross-talk in a human gut inflammation-on-a-chip, Proc. Natl. Acad. Sci. U.S.A. 115 (2018) E10539–E10547.
[80] K. Takov, D.M. Yellon, S.M. Davidson, Confounding factors in vesicle uptake studies using fluorescent lipophilic membrane dyes, J. Extracell. Vesicles 6 (2017) 1388731.